2012

Assessing the Effects of DEM Uncertainty on Erosion Rate Estimation in an Agricultural Field

Samsuzana Abd Aziz
Iowa State University

Brian L. Steward
Iowa State University, bsteward@iastate.edu

Amy L. Kaleita
Iowa State University, kaleita@iastate.edu

Manoj Karkee
Washington State University

Assessing the Effects of DEM Uncertainty on Erosion Rate Estimation in an Agricultural Field

Abstract
The slope length and steepness (LS) factor is one of the factors in the Revised Universal Soil Loss Equation (RUSLE) needed to estimate average annual erosion rate. The LS factor is often derived from digital elevation models (DEM). DEM errors and uncertainty could affect LS factor estimation and consequently erosion rate estimation. However, DEM uncertainties are not always accounted for, and the effects are not always evaluated in erosion rate estimation. This study compared the erosion rate estimation of a 62.81 ha agricultural crop area using a 7.5 min USGS DEM and DEMs developed using real-time kinematic differential GPS (RTK-DGPS) and dual-frequency DGPS (DF-DGPS) field surveys. Spatial estimation and uncertainty analysis was carried out using sequential Gaussian simulation (SGS). A total of 50 equiprobable DEM realizations were produced using SGS to assess DEM uncertainty and quantify its effect on erosion rate estimation. DEM uncertainty substantially affected the resulting erosion rate estimation. The uncertainty of the average annual erosion rate estimates across the study field was represented using 95% confidence intervals (CI). For the DF-DGPS and USGS DEMs, the percentages of the field area that have erosion rate CIs greater than 11.21 Mg ha-1 year-1 (5 tons acre-1 year-1) were 81% and 85%, respectively, which were substantially larger than that of the RTK DEM (0.41%). The average annual erosion rate map produced using a USGS DEM contained artifacts and underestimated the erosion rate estimation in many areas of the field. The results suggested that higher-accuracy DEMs generated using RTK-DGPS measurements are more appropriate for erosion rate estimation in an agricultural field. Knowledge of DEM uncertainty and its effect on the erosion rate estimation was useful to better judge the reliability of erosion rate estimates.

Keywords
Digital elevation model, Erosion rate, Soil loss, Stochastic simulation, Uncertainty assessment

Disciplines
Agriculture | Bioresource and Agricultural Engineering

Comments
This article is from *Transactions of the ASABE*, 55, no. 3 (2012): 785–798.

ASSESSING THE EFFECTS OF DEM UNCERTAINTY ON EROSION RATE ESTIMATION IN AN AGRICULTURAL FIELD

S. Abd Aziz, B. L. Steward, A. Kaleita, M. Karkee

ABSTRACT. *The slope length and steepness (LS) factor is one of the factors in the Revised Universal Soil Loss Equation (RUSLE) needed to estimate average annual erosion rate. The LS factor is often derived from digital elevation models (DEM). DEM errors and uncertainty could affect LS factor estimation and consequently erosion rate estimation. However, DEM uncertainties are not always accounted for, and the effects are not always evaluated in erosion rate estimation. This study compared the erosion rate estimation of a 62.81 ha agricultural crop area using a 7.5 min USGS DEM and DEMs developed using real-time kinematic differential GPS (RTK-DGPS) and dual-frequency DGPS (DF-DGPS) field surveys. Spatial estimation and uncertainty analysis was carried out using sequential Gaussian simulation (SGS). A total of 50 equiprobable DEM realizations were produced using SGS to assess DEM uncertainty and quantify its effect on erosion rate estimation. DEM uncertainty substantially affected the resulting erosion rate estimation. The uncertainty of the average annual erosion rate estimates across the study field was represented using 95% confidence intervals (CI). For the DF-DGPS and USGS DEMs, the percentages of the field area that have erosion rate CIs greater than 11.21 Mg ha^{-1} year^{-1} (5 tons acre^{-1} year^{-1}) were 81% and 85%, respectively, which were substantially larger than that of the RTK DEM (0.41%). The average annual erosion rate map produced using a USGS DEM contained artifacts and underestimated the erosion rate estimation in many areas of the field. The results suggested that higher-accuracy DEMs generated using RTK-DGPS measurements are more appropriate for erosion rate estimation in an agricultural field. Knowledge of DEM uncertainty and its effect on the erosion rate estimation was useful to better judge the reliability of erosion rate estimates.*

Keywords. *Digital elevation model, Erosion rate, Soil loss, Stochastic simulation, Uncertainty assessment.*

Soil erosion is one of the most important agricultural management problems. Water erosion is the detachment and transport of soil from land by water, including runoff from melted snow and ice. Topography is a major factor affecting soil erosion by water (Fangmeier et al., 2006). Naturally, a higher degree of slope in the field causes greater soil loss due to water erosion. Soil erosion by water also increases as the slope length increases due to the greater accumulated runoff and energy in the moving water.

In the 1960s, the Universal Soil Loss Equation (USLE) was developed to estimate soil erosion by water primarily for croplands. USLE is based on empirical relationships derived from experimental data collected from the 1940s to the 1970s and is implemented through the use of tables, figures, and nomographs (Wischmeier and Smith, 1965). Later, the Revised Universal Soil Loss Equation (RUSLE1), a software version of an improved USLE for any land uses, was released in the early 1990s (Renard et al., 1997) followed by RUSLE2 in 2003 (USDA, 2008). Generally, RUSLE estimates long-time average annual soil loss based on six factors, including rainfall erosivity, soil erodibility, slope length, slope steepness, cover management, and support practices. RUSLE accounts for topographic effects through the product of the slope length (L) and steepness (S) subfactors, which when combined are called the topographic factor, or the LS factor. The LS factor represents the ratio of soil loss on a given slope length and steepness to soil loss from a slope that has a length of 22.13 m and a uniform steepness of 9% where all other factors are the same (McCool et al., 1997).

Topographic data are therefore important for estimating soil erosion and are often extracted from digital elevation models (DEMs). Many environmental studies have used DEMs to derive the LS factor in erosion risk estimation. Lu et al. (2004), for example, mapped soil erosion risk in a large area of the Brazilian Amazonia forest using RUSLE with a 30 m DEM digitized from a 1:100,000 topographic map. They found that the majority of the study area had LS values less than 2.5, and most of the forest area had low erosion risk. Hoyos (2005) created a 25 m resolution DEM from a contour map of a 52 km^2 coffee-growing region in Colombia to calculate the LS factor for soil erosion estimation in that area. They found that the relationship between the LS factor and soil erosion potential had a correlation coefficient (Spearman r) ranging from 0.57 to 0.59, indicat-

Submitted for review in January 2011 as manuscript number SW 9017; approved for publication by the Soil & Water Division of ASABE in May 2012.

The authors are **Samsuzana Abd Aziz, ASABE Member,** Senior Lecturer, Department of Biological and Agricultural Engineering, Universiti Putra Malaysia, Serdang, Malaysia; **Brian L. Steward, ASABE Member,** Professor, and **Amy Kaleita, ASABE Member,** Associate Professor, Department of Agricultural and Biosystems Engineering, Iowa State University, Ames, Iowa; and **Manoj Karkee, ASABE Member,** Assistant Professor, Department of Biological Systems Engineering, Washington State University, Prosser, Washington. **Corresponding author:** Samsuzana Abd Aziz, Department of Biological and Agricultural Engineering, Faculty of Engineering, Universiti Putra Malaysia, 43400 UPM Serdang, Selangor Darul Ehsan, Malaysia; phone: +603-8946-4326; e-mail: suzana@eng.upm.edu.my.

  ISSN 2151-0032

ing evidence of topographic influence on soil erosion potential in that area. Lee and Lee (2006) generated a 20 m resolution DEM of the 274 km^2 Bosung basin in Korea by digitizing and interpolation of contour lines on a 1:5000-scale topographic map. They used the DEM as a parameter input to RUSLE. Their study implied that the topographic LS factor, which is directly derived from the DEM, is sensitive to grid size. The optimal resolution to quantify soil loss in the RUSLE model for the study site was 125 m.

These studies demonstrated the use of DEMs for soil erosion estimation in environmental studies over large-scale areas (watershed scale). For a relatively smaller scale (field scale), a reliable field DEM is vital because estimation of LS from an unreliable DEM could propagate errors into soil loss estimates, which could lead to a poor assessment of conservation practices in agricultural fields. Renschler and Flanagan (2008) used a real-time kinematic differential GPS (RTK-DGPS) survey and six alternative elevation data sources for soil erosion assessments using the Water Erosion Prediction Project (WEPP) model. They found that the more precise topographic measurements with a RTK-DGPS, a photogrammetric survey (TIN), and DGPS yielded more precise on-site soil loss estimates at all scales ranging from individual raster cells (0.01 ha) and hillslope areas (0.5 ha) to small watersheds (>4 ha). They also found that DEMs based on U.S. Geological Survey (USGS) 10 ft contour lines from publicly available data can be as good as the most accurate datasets (RTK-DGPS or TIN) in estimating average annual off-site runoff (-18.3% error) and sediment yield (-2.7% error) using the WEPP model within a 30 ha watershed. They demonstrated that not only the accuracy of the data source but also the appropriate handling and consequent analysis of topographical data within the GIS model environment have an impact on useful estimation results.

Existing publically available USGS DEMs or more accurate measurements collected from GPS-aided farm operations can be used to generate a field-scale DEM (Renschler and Flanagan, 2008). Depending on the data sources, methods, and procedures used to generate the field DEMs, the DEM estimates contain errors (Holmes et al., 2000; Wechsler and Kroll, 2006; Weschler, 2007). DEM errors affect LS factor estimation (Renschler et al., 2001) or any other DEM-derived parameters (Weschler, 2007). Although this effect is well known, DEMs are often used as the true field surface, and the topographical uncertainty is not always accounted for in such applications.

The root mean square error (RMSE), the typical global measure of DEM accuracy, does not provide an accurate assessment of how precisely each grid in a DEM represents topographical features (Wise, 1998; Wechsler, 2007). Hence, a number of researchers have investigated spatial simulation methods to assess the uncertainty of elevation estimates in each DEM grid (Hunter et al., 1995; Holmes et al., 2000; Carlisle, 2005; Wechsler and Kroll, 2006). The simulation process accounts for spatial correlation in the data to produce equiprobable estimates (realizations) for each particular grid in the DEM. These realizations provide a range within which the true estimate lies and can be used to quantify the uncertainty at each DEM grid (Wechsler, 2007).

It is important to assess the uncertainty associated with DEM elevation estimates, so that the propagation of these errors can be accounted for in other derived parameters or models. In this study, a 7.5 min USGS DEM and GPS field measurements were used to develop field-scale DEMs from which LS factors were calculated and average annual erosion rate was estimated for an agricultural field. The objectives of this study were to (1) assess the uncertainty in field DEM elevation estimates and their effect on erosion rate estimation, and (2) compare erosion rate uncertainty calculated using a USGS DEM and DEMs developed from GPS field surveys.

Materials and Methods

Elevation Data and DEM Development

The study field was located in Boxholm, Iowa, and covered a 62.81 ha (795 m wide × 790 m long) agricultural crop area. The field elevation ranged from 1140 to 1162 m (22 m elevation difference), and the slope ranged from 0% to 30%. Elevation data (7097 points) were collected during a seeding operation using an agricultural implement equipped with a RTK-DGPS receiver (StarFire RTK, Deere & Co., Moline, Ill.) with a vertical static RMSE of less than 0.025 m. Another set of elevation measurements (6874 points) was collected using a dual-frequency DGPS (DF-DGPS) receiver (StarFire SF2, Deere & Co., Moline, Ill.) mounted on a John Deere harvester during a harvesting operation. The DF-DGPS receiver had a vertical static RMSE of around 0.1 m. For both field operations, the vehicle traveled along 10 m swaths in the east-west direction.

A 7.5 min USGS DEM of Boxholm, which is located in Boone County, Iowa, was acquired from an online GIS data provider (GeoCommunity, 2007). This DEM covered an area of 147.11 km^2, had a 30 m cell resolution, and was generated by contour digitization, with a rated vertical RMSE of 7.0 to 15.0 m. At least 28 test points within the DEM (20 interior points, 8 along the edges) located at benchmarks, spot elevations, or points on contours from existing source maps were used by the USGS to calculate the RMSE (USGS, 1998). The DEM has an absolute vertical elevation error tolerance of 50 m for any grid node when compared to the test points. The USGS has set a standard that any array of points in the DEM cannot encompass more than 49 contiguous elevations to have error greater than 21 m. The 0.63 km^2 portion of the USGS DEM (6874 points) within the boundary of the field was used in this study.

Exploratory data analysis was done to study and understand the characteristics of the elevation measurements in each dataset. The GPS measurement histograms were slightly skewed to the left although the distribution was generally normal, indicating that a small percentage of measurements had high elevations (figs. 1b and 1d). The USGS dataset histogram revealed a strongly multimodal distribution (fig. 1f) as a result of the sparse pattern of elevation data points, which failed to capture the continuity and surficial detail in the field topography. There were low elevation patterns in the middle and southwest region of the study field that were smoothed in the USGS dataset (fig.

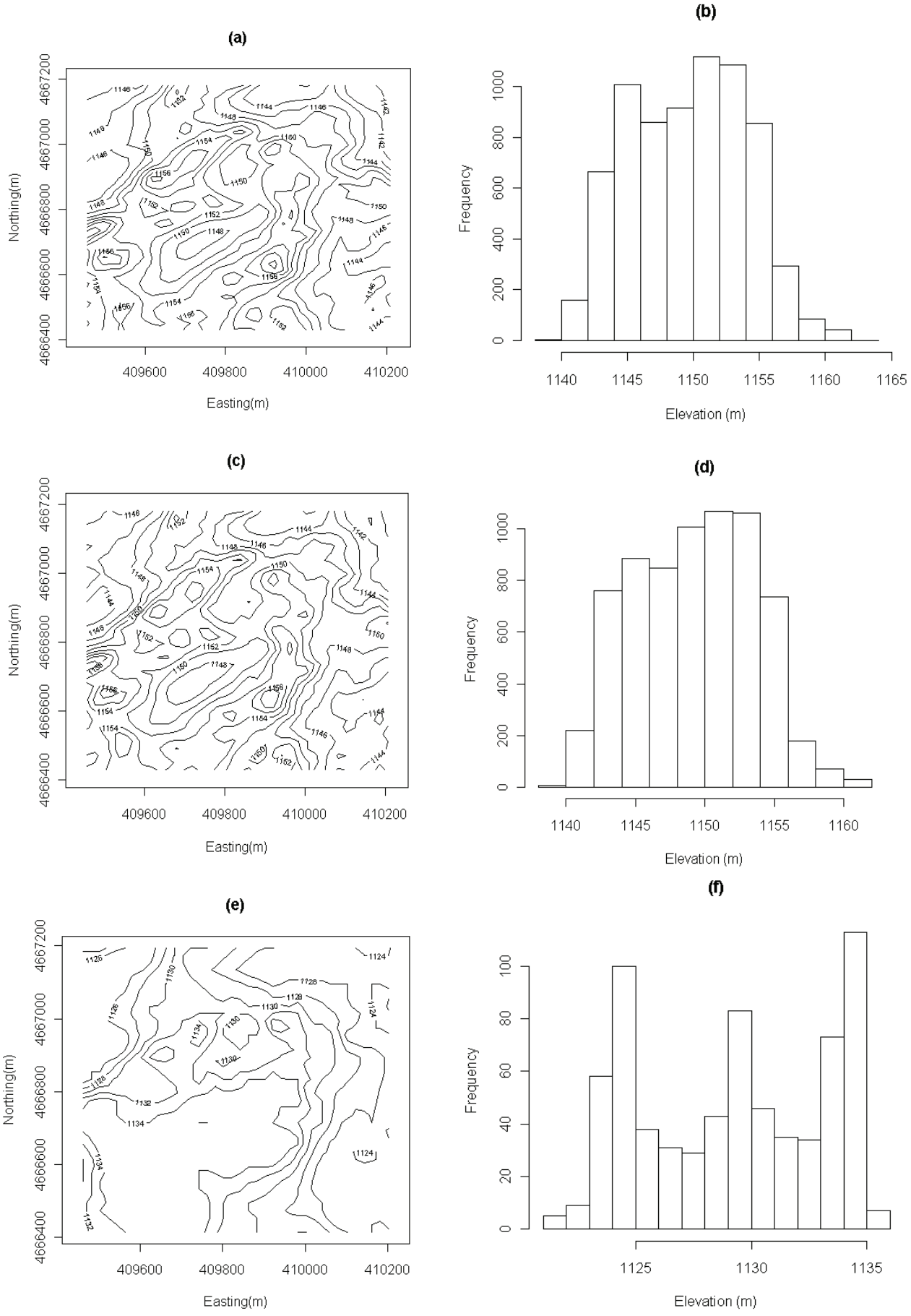

Figure 1. Contour maps and histograms of the elevation data consisting of (a and b) 7097 points from RTK-DGPS measurements, (c and d) 6874 points from DF-DGPS measurements, and (e and f) 704 points from the USGS DEM.

1e). The USGS dataset also underestimated the elevation, as the USGS values ranged from 1121 to 1136 m, about 20 m lower in average than the GPS measurements (ranged from 1139.6 to 1162.0 m). This may have been due to systematic errors as a result of the procedures used in the USGS DEM generation process that cause bias in the elevation. The USGS DEM was then co-registered to the RTK-DGPS elevation measurements by shifting up the USGS elevation by 20 m to eliminate these errors. From this point forward, the USGS co-registered elevations were used for further analysis.

Using each elevation dataset, field-level DEMs were developed. This process included interpolating the GPS measurements and the 30 m USGS DEM into 10 m gridded DEMs. For synchronization, the locations of the DEM grids were pre-defined so that each DEM developed using different datasets would use the same grid locations. The synchronization was done to ensure that the raster grids for the various DEMs precisely overlaid each other and that the values could be compared to each other in the later analysis.

Elevation data were interpolated using ordinary kriging to generate the DEMs of the field. Ordinary kriging was chosen because it is a commonly used unbiased estimator that seeks to minimize error variance (Isaaks and Srivastava, 1989), which provides the best estimate of the value based on the available data. In addition, visual inspection of the data indicated no large trends, and ordinary kriging is known to be quite robust (Trangmar et al., 1985). The *gstat* program in R statistical software (Free Software Foundation, Inc., Boston, Mass.) was use to perform the interpolation.

The sample semivariogram of each dataset was fit with a Gaussian semivariogram model because a Gaussian model presents a region of low slope near the zero distance, which is suitable for data that vary smoothly, such as elevation data. The semivariogram models for RTK and DF-DGPS measurements were similar, with a small nugget value of 0.1 m^2. For the USGS DEM data, the semivariogram had a nugget value of 0.6 m^2 (fig. 2). The nugget values provide an indication of the amount of local variation in the dataset, or an indication of the micro-spatial variability at a scale below the sampling resolution.

Using the semivariogram models, elevation data from each dataset were interpolated. A fixed radius of 60 m and a minimum of 30 data points were used to ensure enough interpolation support within an applicable computation time.

Error Simulation of DEMs

Error simulation enables quantification of uncertainty associated with elevation estimates and its derived parameter in each DEM grid. In this section, the procedure to assess elevation estimates uncertainty is discussed.

Researchers have used error measured at discrete points (such as from GPS surveys or data of higher resolution) to estimate and investigate DEM error and the spatial structure of the DEM error (Holmes et al., 2000; Carlisle, 2005; Karkee et al., 2008). In this study, DF-DGPS measurements and USGS datasets had lower accuracy relative to the RTK-DGPS measurements. Therefore, the RTK-DGPS elevation measurements were used as reference measurements to calculate errors contained in lower-accuracy datasets. The error was calculated by subtracting the nearest-neighbor RTK-DGPS elevation measurement from the interpolated elevation at each DF-DGPS and USGS DEM grid.

The DF-DGPS errors had no visible spatial patterns (fig. 3a). The histogram of the error values from the DF-DGPS dataset followed a roughly normal distribution, with a mean of -0.44 m, a median of -0.42 m, and a standard deviation of 0.69 m, indicating that, on average over the study area, the DF-DGPS DEM underestimates the elevation by -0.44 m (fig. 3b). However, the maximum error value of 3.14 m and minimum of -4.76 m show there are large differences from RTK-DGPS measurements in some areas. The semivariogram of the DF-DGPS error data shows some spatial correlation, and there is a slight trend of increasing variance with distance to a 200 m range (fig. 3c).

The USGS DEM error exhibited spatial patterns; particularly visible was a large region (area of topographic depression in the RTK-DGPS DEM) with positive error values up to around 8 m (fig. 3d). There were also several small regions in which negative error was observed. These regions were typically larger than the underlying 30 m spatial resolution of the original DEM. The USGS co-registered DEM error histogram was slightly skewed to the

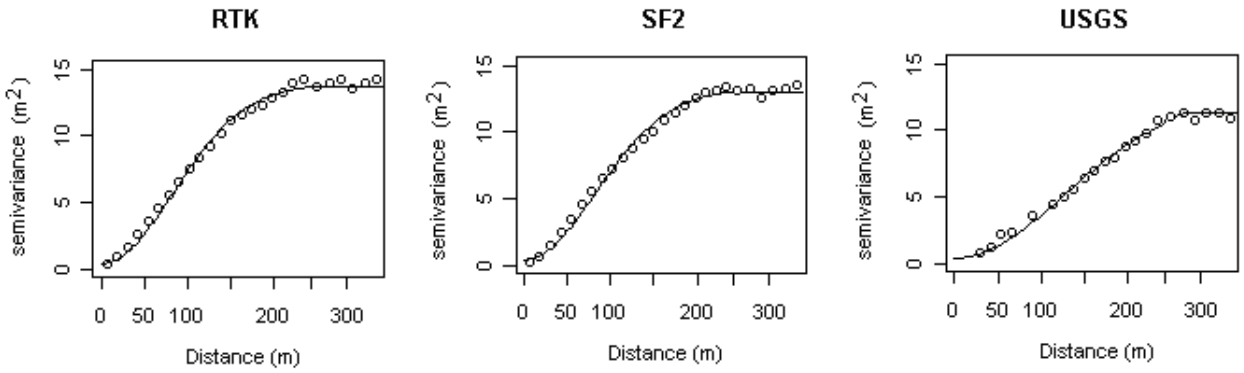

Figure 2. Semivariograms of RTK-DGPS and DF-DGPS measurements and USGS DEM data. The solid line on each semivariogram is the semivariogram model generated using the *gstat* program in R statistical software.

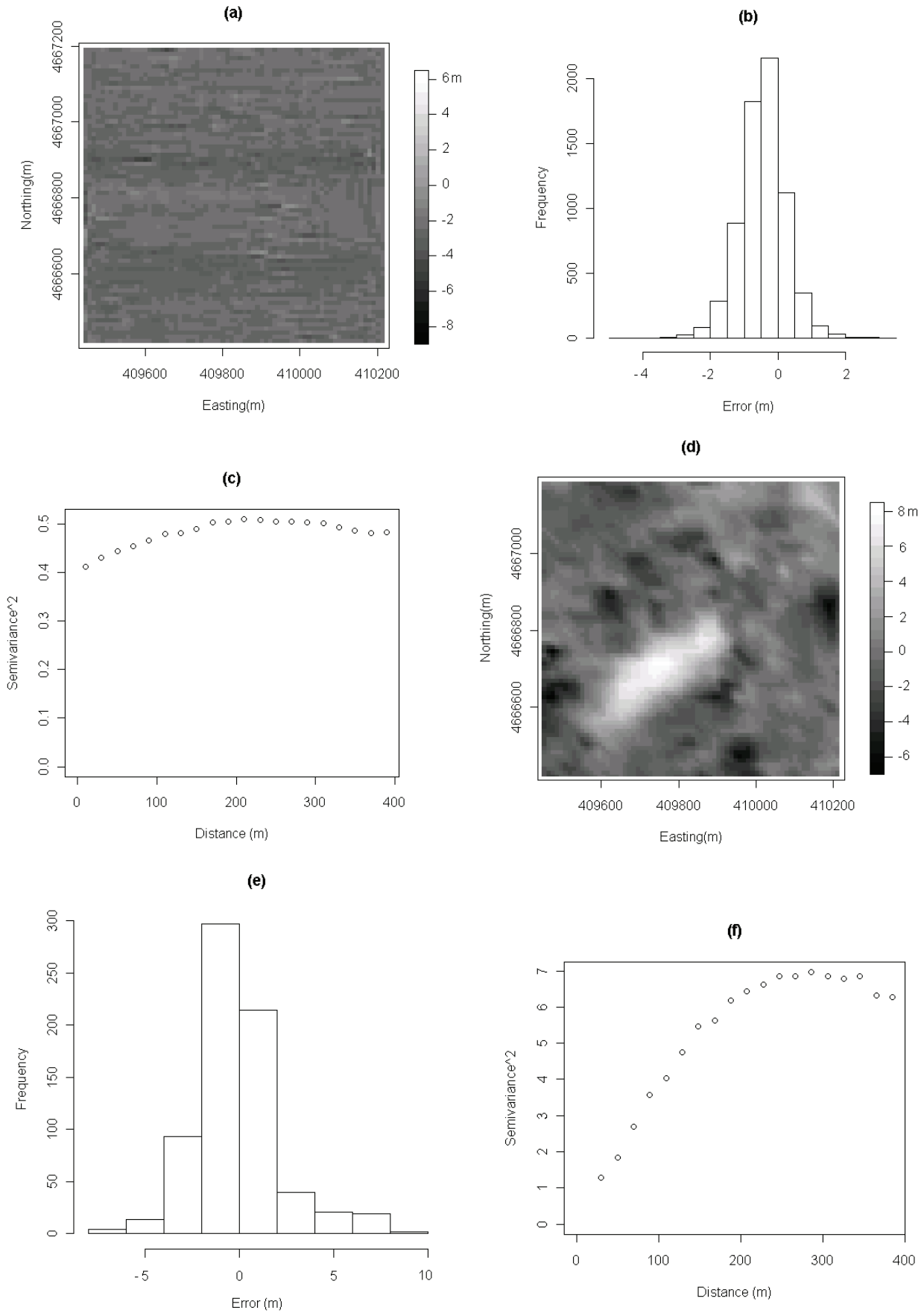

Figure 3. Plots and histograms of (a and b) 6874 points of DF-DGPS measurement error and (d and e) 704 points of USGS DEM error with (c and f) their corresponding semivariograms.

left, indicating that a high percentage of grids underestimated the elevation value. Across the field, the mean error was -0.11 m, the median was -0.25 m, and the standard deviation was 2.28 m. The maximum (8.45 m) and the minimum (-7.04 m) error values show that there are significant differences in some areas. The semivariogram of the USGS DEM error data shows spatial correlation with a substantial increase in variance with increasing distance to a 200 m range (fig. 3f).

Many studies have shown that DEM error is spatially variable (Ehlschlaeger and Shortridge, 1997; Hunter and Goodchild, 1997; Carlisle, 2005) and spatially correlated. Therefore, a model of DEM error should not be random, but spatially dependent. In this study, the magnitude and spatial distribution of error in the DEMs was evaluated using a geostatistical method that is recognized to be a realistic approach for DEM error modeling because it provides alternative plausible representations of possible spatial distribution of errors in a DEM (Holmes et al., 2000).

Sequential Gaussian simulation (SGS) was used to produce multiple realizations of error values at each DEM grid based on available error data and spatial distribution of the error. Detailed descriptions of the SGS algorithm can be found in Goovaerts (1997). The SGS was implemented using the *gstat* program in R (Free Software Foundation, Inc., Boston, Mass.). Prior to the simulation process, the normal scores transform, a non-linear transform that remaps any distribution to a normal distribution (Goovaerts, 1997), was applied to the error datasets to map the error distribution into a standard normal distribution. This transformation was done to meet the format requirement of Gaussian simulation, which is that the univariate distribution of the error data be standard normal (figs. 4a and 4c). The semivariogram of the normal score-transformed error data was modeled for simple kriging estimation used in the simulation routine. Using *gstat*, the DF-DGPS normal score-transformed error data were fit with a spherical semivariogram model with a nugget effect of 0.8 m^2, lag distance of 180 m, and sill of 1.0 m^2 (fig. 4b). The USGS normal score-transformed error data were fit with a spherical semivariogram model with a nugget of 0.3 m^2, lag distance of 200 m, and sill of 1.2 m^2 (fig. 4d).

SGS models the uncertainty in the error data based on the normal score-transformed data available near each point of the DEM grids. The simple kriging estimates (kriging prediction and its associated kriging variance) were used to

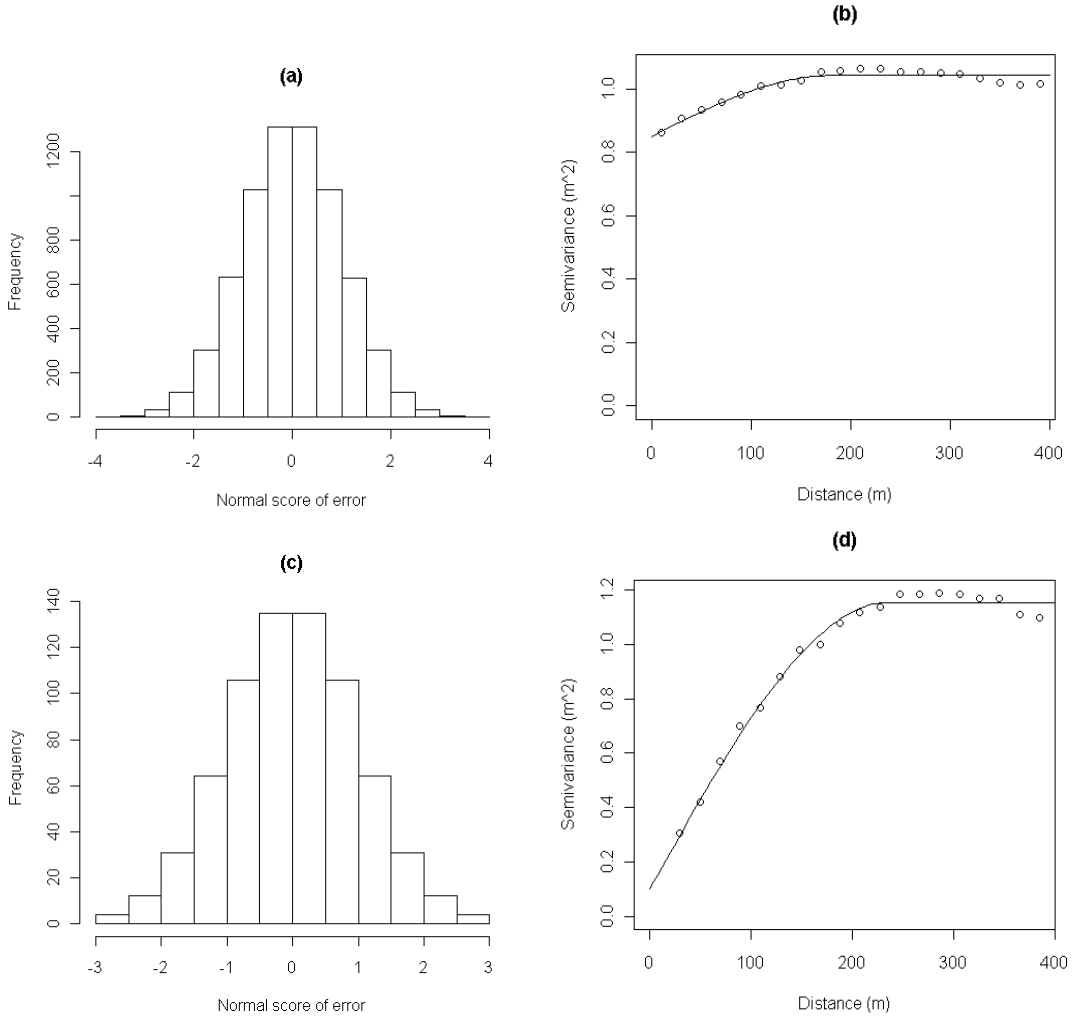

Figure 4. Histograms of the normal score-transformed data of (a) 6874 points of DF-DGPS measurement error and (c) 704 points of USGS DEM error with (b and d) their corresponding semivariograms. The solid line on each semivariogram is the semivariogram model.

establish the local conditional cumulative distribution function (ccdf) of the error estimates at every DEM grid location. Within the simulations, multiple realizations of error predictions were randomly drawn from the ccdf. Once the simulations of the normal score values have been produced, each realization must be back-transformed to the original error distribution. This process essentially consists of taking the inverse of the normal scores transform to remap the normal score distribution to the original error histogram.

A total of 50 simulations were run, resulting in 50 realizations of each DEM error map. The minimum number of needed simulations was determined when the percent difference in standard deviation of simulated errors between subsequent simulations was below 1% and reached a steady state. The final step of the uncertainty analysis was to add the simulated error realizations of each dataset to its original kriged DEM. This created 50 equiprobable DEM realizations for each dataset to be used for erosion rate estimation. These realizations provide a range within which the true estimate lies and can be used to quantify elevation uncertainty associated with each DEM and its effect on erosion rate estimation.

For the RTK-DGPS measurements, the vertical RMSE of the receiver was stated to be less than 0.025 m by the GPS receiver manufacturer. Typically, in the absence of higher-accuracy data to calculate error values, a global accuracy measure such as RMSE is the only statistic available. When RMSE is the only information available, DEM errors are often modeled based on a random process of error values with standard deviation equal to the RMSE value (Weschler, 2007), which means that the DEM error is assumed to be spatially uncorrelated. This assumption is generally not appropriate for modeling error in DEMs because higher error is expected in areas of more rugged terrain (Hunter and Goodchild, 1997). Indeed, a number of authors reported that DEM errors could be larger on steep slopes (Hunter and Goodchild, 1997; Carrara et al., 1997), lower in less complex terrain (Gao, 1997), correlated with terrain ruggedness (Kyriakidis et al., 1999) and gradient, and could be related to other elevation features (Ehlschlaeger and Shortridge, 1997). As the RTK-DGPS measurements were collected using a moving vehicle, the assumption that the elevation errors were related to terrain variability seems appropriate because measurement errors due to vehicle dynamics resulted from the vehicle interaction with field topography or variability in the field surface.

Hence, the methodology presented here is intended to model the RTK-DGPS DEM errors based on the known RMSE and relate it to the elevation variability. The spatial distribution of RTK-DGPS DEM error related to the elevation variability was assessed using SGS. The normal score transform of the RTK-DGPS elevation measurements were used within the simulation to produce 50 realizations of elevation values at each DEM grid. First, the spatial correlations in the normal score-transformed data were modeled using a Gaussian semivariogram model with a nugget value of 0.1 m^2, similar to that of the original elevation. After simulation, the elevation realizations were back-transformed to the original elevation data distribution. This produced 50 DEM realizations, which were then subtracted from the mean realizations to produce 50 realizations of error maps. Each error map provides a plausible representation of possible spatial distribution of errors in the DEM, in which the spatial structure related to elevation variability was accounted for within the SGS routine (fig. 5). As the RMSE of the RTK-DGPS measurements was 0.025 m, the error maps were rescaled to have mean value equal to zero and standard deviation equal to the RMSE of the RTK-DGPS measurements of 0.025 m. The rescaled error maps were added to the previously kriged RTK-DGPS DEMs to produce 50 equiprobable RTK-DGPS DEMs for erosion rate estimation. These realizations provide a range within which the true estimate lies and can be used to quantify the RTK-DGPS DEM uncertainty and its effect on erosion rate estimation.

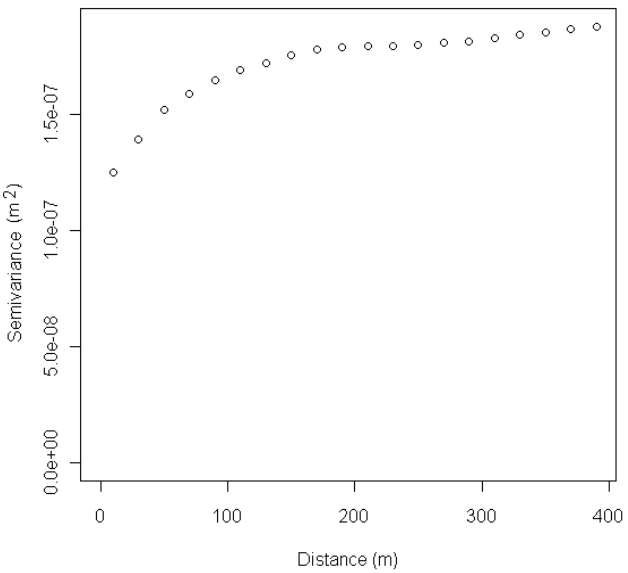

Figure 5. Semivariogram showing the spatial correlation of RTK-DGPS DEM errors produced using sequential Gaussian simulation.

EROSION RATE ESTIMATION USING RUSLE

The LS topographical factor estimates were derived from the 50 realizations of DEMs from each dataset using ArcView (version 3.3, ESRI, Redlands, Cal.) within the ArcView Spatial Analyst extension. The calculation was done using an Avenue script of *RUSLE3D*, an improved method for RUSLE calculation within GIS (Mitasova et al., 2001). The computation of the LS factor at a point $\mathbf{r} = (x, y)$ is given by:

$$LS(\mathbf{r}) = 1.8 \times [A(\mathbf{r})/22.13]^{0.4}[\sin b(\mathbf{r})/0.09]^{1.4} \quad (1)$$

where $A(\mathbf{r})$ is the upslope contributing area per unit contour width (m^2 m^{-1}), and b is the slope (in degrees).

This process resulted in 50 LS factor maps for each dataset, which were used to produce 50 equiprobable maps of the average annual erosion rate of the field. The annual erosion rate maps were generated by multiplying the LS factor maps with other RUSLE factors, as follows:

$$E = R \times K \times LS \times C \times P \quad (2)$$

where

E = estimation of average annual erosion rate caused by sheet and rill erosion (Mg ha^{-1} $year^{-1}$)

R = rainfall erosivity factor for Boone County, Iowa

(2723.2 MJ mm ha^{-1} h^{-1}year^{-1})

K = soil erodibility factor map

LS = slope length and steepness factor maps calculated in ArcView

C = cover and management factor (0.24 for corn-soybean rotation with spring conservation tillage)

P = support practice factor (1, indicating no soil conservation practice).

The soil erodibility factor map was developed based on the soil database generated by the USDA Natural Resource Conservation Service (NRCS) and distributed with the RUSLE2 software. RUSLE2 is a RUSLE model-based software package developed by the USDA Agricultural Research Services (ARS). A collection of dynamically linked RUSLE2 libraries called RomeDLL was also developed and distributed with RUSLE2 software. In this study, RomeDLL was incorporated into a custom-developed application to extract soil type and corresponding erodibility value for each DEM grid within the two test fields. Six different soil types were present in the test fields: Canisteo silty clay loam, Okoboji mucky silt loam, Harps loam, Nicollet loam, Clarion loam, and Crippin loam. Erodibility factors among these loam variations varied from 0.032 to 0.042 MG ha h MJ^{-1} ha^{-1} mm^{-1}.

Uncertainty Assessment Method

Using 50 elevation realizations and the resulting 50 erosion rate realizations from the three DEM sources, the uncertainty of the estimates in each grid was quantified. The elevation and erosion rate uncertainty in each grid were based on the dispersion of the estimates from their mean. The dispersion was estimated by calculating the 95% confidence interval (CI) of the estimate in each grid, indicating 95% probability that the mean of the estimates falls in that interval. The 95% CI was calculated as the standard deviation multiplied by the critical two-tailed value of 1.96 for a standard normal distribution (Sheskin, 2004):

$$z_i = \pm 1.96\sigma_i \quad (3)$$

where z_i refers to the lower and upper 95% CI of the estimates in the ith grid, with i as the indexing number of the grid across the map, and σ_i refers to the standard deviation of the estimates in ith grid. The 95% CI estimator provides an indication of statistical dispersion of the estimated parameters, which can be used to quantify the uncertainty of the estimated parameter at each grid location. An estimate with a small CI is more reliable than an estimate that has a large CI. By calculating the CI in each grid estimate across the map, the estimated spatial uncertainty at any particular location can be observed and studied.

Results and Discussion

Simulated DEMs

Contour plots of the DEMs developed using each elevation dataset showed that the field generally has lower elevations at its southeast, northeast, and northwest edges (fig. 6). There were some common patterns with dense contour lines in several spots, indicating high elevation gradients

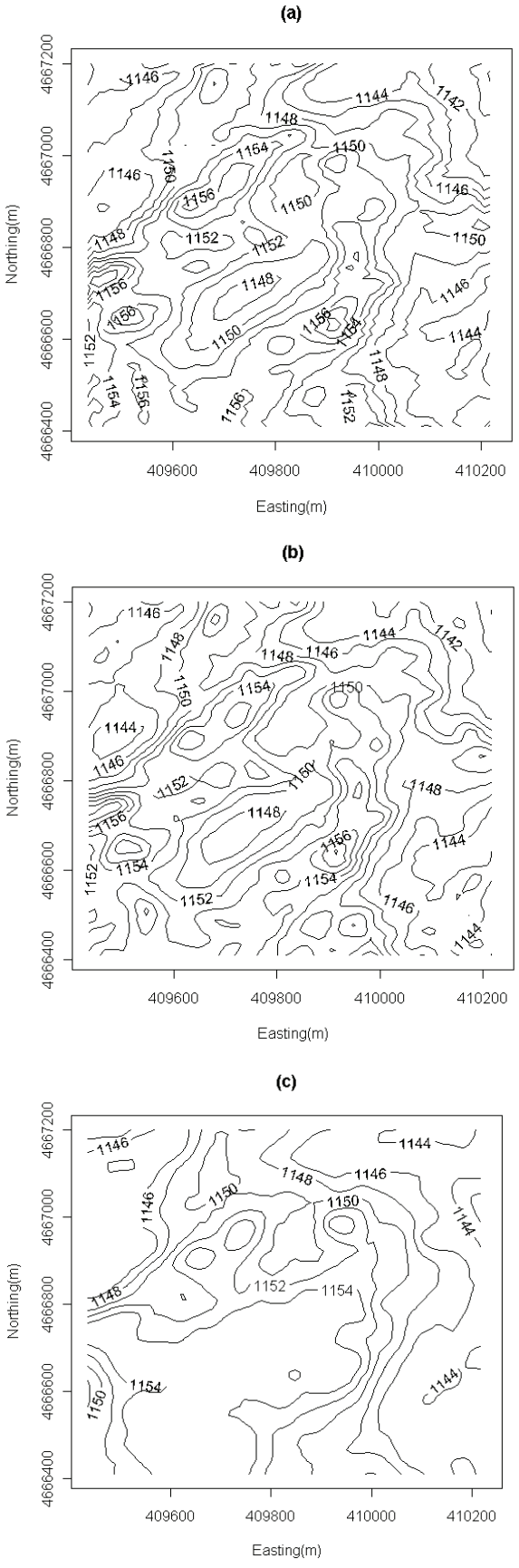

Figure 6. Contour plots of the kriged DEMs developed using (a) RTK-DGPS measurements, (b) DF-DGPS measurements, and (c) USGS DEM dataset.

Table 1. Summary statistics of 50 equiprobable elevations and erosion rate across the study field.

		Elevation Across Field (m)				Erosion Rate Across Field (Mg ha^{-1} year^{-1})			
	Dataset	Mean (μ)	Range	5th %	95th %	Mean (μ)	Range	5th %	95th %
Mean	RTK	1149.95	21.63	1143.05	1156.23	10.22	139.41	0.00	36.10
	DF-DGPS	1149.93	21.57	1143.01	1156.22	10.07	89.27	1.03	25.93
	USGS	1149.74	21.84	1142.69	1156.07	10.58	96.85	1.57	2.13
95% CI	RTK	0.08	0.14	0.04	0.11	0.54	8.09	0.00	0.21
	DF-DGPS	1.35	2.93	1.05	1.62	23.16	83.74	3.86	46.52
	USGS	1.72	3.40	1.16	3.30	27.67	109.81	5.52	60.10

(figs. 6a and 6b). These patterns appeared differently in the 10 m DEM developed with the USGS data (fig. 6c). The low-resolution USGS DEM data missed many topographical details in the field. Errors as a result of the procedures used in the USGS DEM generation process smoothed the topographic depression in the middle and southwest regions of the field.

In the simulation process, 50 simulated error realizations were added to the kriged DEMs to created 50 equiprobable realizations of the DEMs. The average elevations across the field were calculated by taking the average of all the grid mean elevations across the DEM. Overall, for each of the DEMs, the average estimated elevation was very similar, around 1149.74 to 1149.95 m (table 1). The elevation range was 21.84 m for the USGS DEM, 21.57 m for the DF-DGPS DEM, and 21.63 m for the RTK DEM. The differences in elevation ranges indicate the differences in estimated field DEM elevations from each of the datasets.

Uncertainty Estimates of DEMs

Gray-scale maps of the 95% CI of the elevation estimates in each grid were constructed to describe the uncertainty in the estimated elevation of the DEMs (fig. 7). Darker color indicates higher CI values, which signify higher uncertainty in the estimates. For the DEMs simulated from the RTK-DGPS measurements, the 95% CIs of the grid elevation were very small, with a maximum of 0.15 m (fig. 7a). The small uncertainty was mainly related to the variability in the RTK-DGPS elevation measurements around the grid. The uncertainty can also be related to vehi-

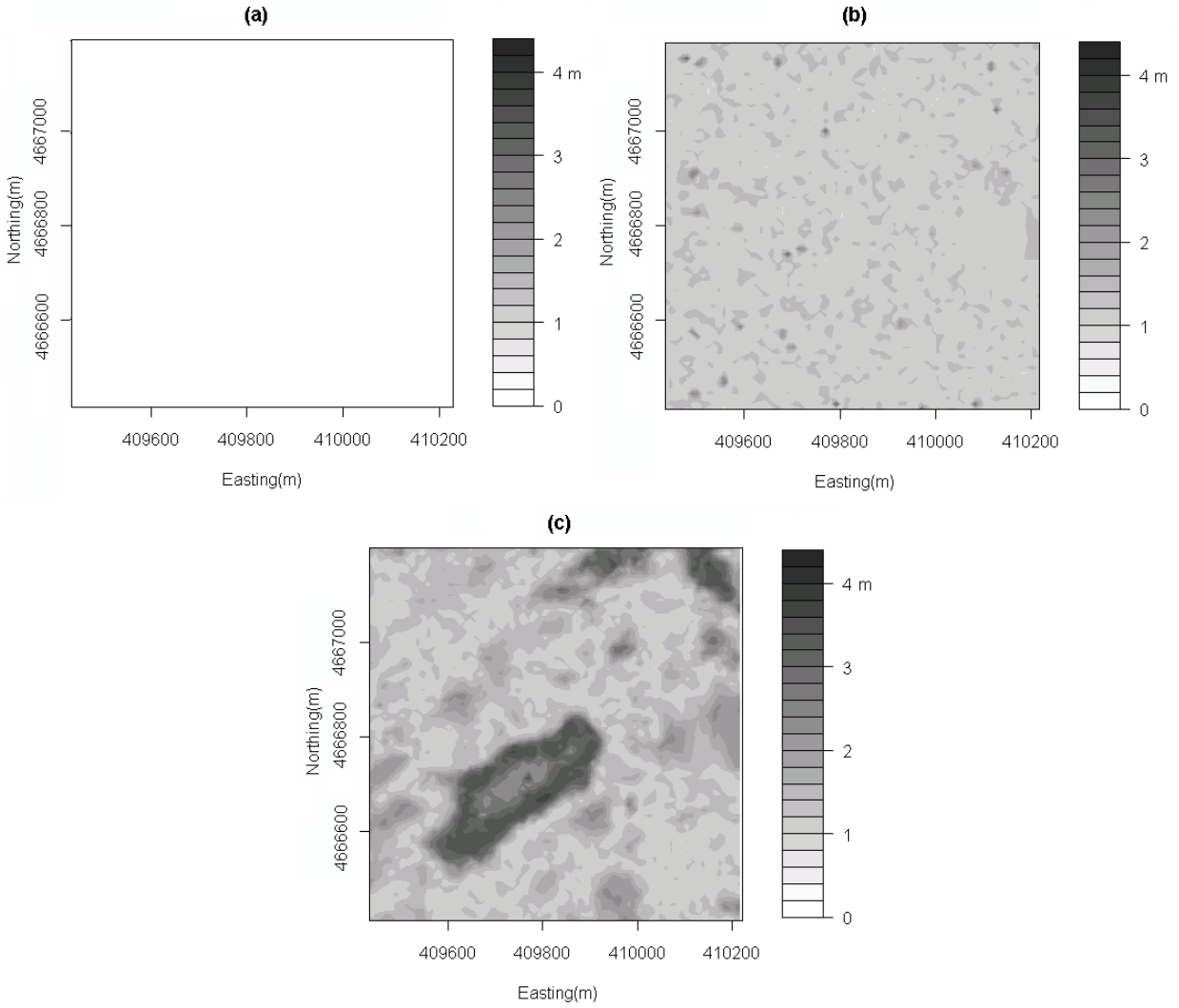

Figure 7. Gray-scale maps of 95% CI for 50 equiprobable DEMs elevations using (a) RTK-DGPS measurements, (b) DF-DGPS measurements, and (c) USGS DEM dataset.

cle dynamics, resulting from the vehicle's interaction with the micro-scale variability in the field surface. For the DEMs simulated from the DF-DGPS measurements, the uncertainty of the simulated elevations in each grid was higher than the RTK DEM, with 95% CI up to 3.12 m (fig. 7b). A few dark patches in some spots of the 95% CI map show that there was a substantial deviation of the DF-DGPS elevations from the RTK DEM, which indicates high uncertainty in that area. The uncertainty in the elevation estimates was more clearly distinguished in the 95% CI map of the DEMs simulated from the USGS dataset (fig. 7c). High values of the 95% CI in the grid elevation estimates were clearly observed in areas with large elevation errors as computed in the error analysis. These areas were characterized in the northeast, middle, and southwest regions of the study field, with 95% CIs up to 4.33 m. Small estimated elevation CIs in the RTK DEM grids show that the degree of certainty in the grid elevation was higher using the RTK-DGPS measurements compared to the DF-DGPS measurements and USGS dataset. The uncertainty estimates could give some insight to help the modeler understand the uncertainty of the subsequent analyses that use data derived from a specific DEM.

Overall across the study field, the average uncertainty of the grid elevation estimate was highest for the USGS DEM (table 1). The average 95% CIs of the mean simulated elevation values in each grid across the field study for the RTK DEM, DF-DGPS DEM, and USGS DEM were 0.08 m, 1.35 m, and 1.72 m, respectively. The range of CIs across the field was 0.14 m for RTK DEM, 2.93 m for DF-DGPS DEM, and 3.48 m USGS DEM. Although the difference in elevation between the DF-DGPS DEM and RTK DEM was smaller compared to the difference in elevation between the USGS DEM and RTK DEM (fig. 3), the range of 95% CIs across the DF-DGPS DEM was relatively high, indicating that there was high uncertainty in some areas.

It is the responsibility of the modeler to determine whether the uncertainty in these DEMs will affect the results of applications that use the parameters derived from the DEMs. The effect of the DEM uncertainty on average annual erosion rate estimation of the field is discussed in the following section.

Estimated Average Annual Erosion Rate

The estimated average annual erosion rates for kriged DEMs using GPS measurements were similar to each other (figs. 8a and 8b). As expected, higher values of estimated erosion rate were observed in areas with higher slope values. The highest erosion rate values appeared in a few spots with the highest peak in the west part of the field. The contour pattern of erosion rate estimates derived from the kriged DF-DGPS DEM (fig. 8b) showed similarity with the erosion rate pattern from the RTK DEM (fig. 8a), although most of the high erosion rate areas were underestimated. For the USGS DEM, the areas that have high elevation uncertainty characterized in the previous section (in northeast, middle, and southwest) were the areas that have the most differences in erosion rate estimation relative to the erosion rate estimates derived from the RTK DEM (fig. 8c).

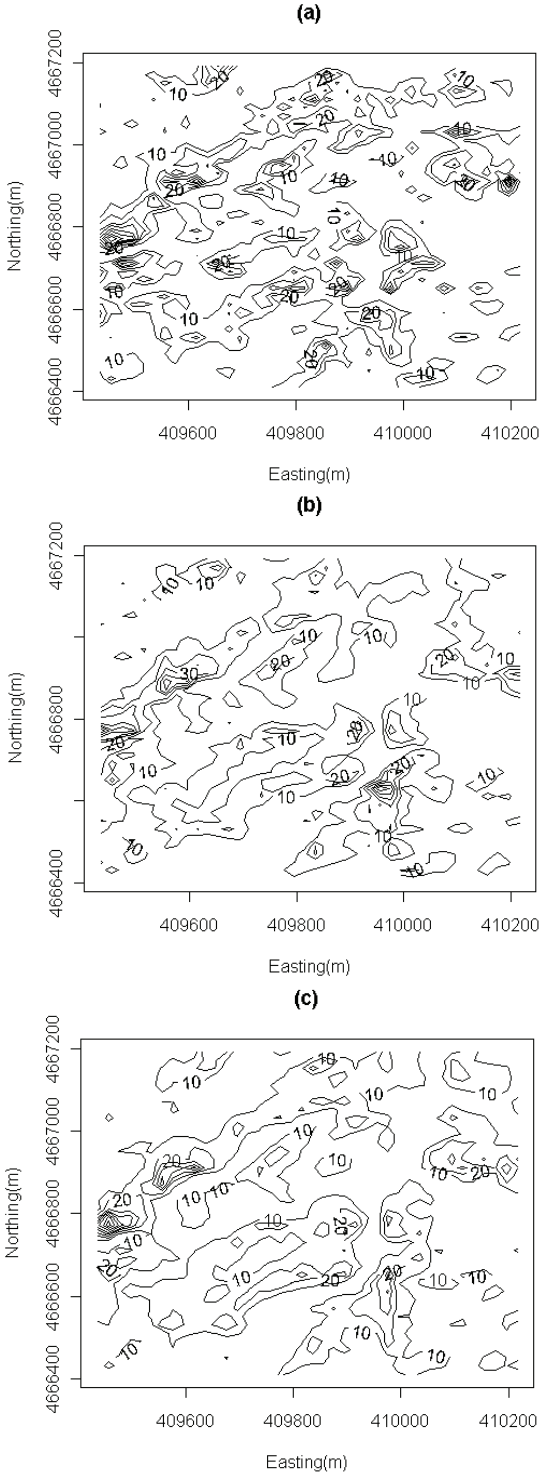

Figure 8. Contour map of erosion rates in Mg ha^{-1} year^{-1} calculated from kriged DEMs using (a) RTK-DGPS measurements, (b) DF-DGPS measurements, and (c) USGS DEM dataset.

The mean of the simulated average annual erosion rates across the field was calculated by averaging all the mean erosion rates across the entire DEM. For each DEM, the average annual erosion rate for the whole field was very similar and ranged from 10.07 to 10.58 Mg ha^{-1} year^{-1} (table 1). However, the range of average annual erosion rate across the field for the RTK DEM was 139.41 Mg ha^{-1} year^{-1}, which

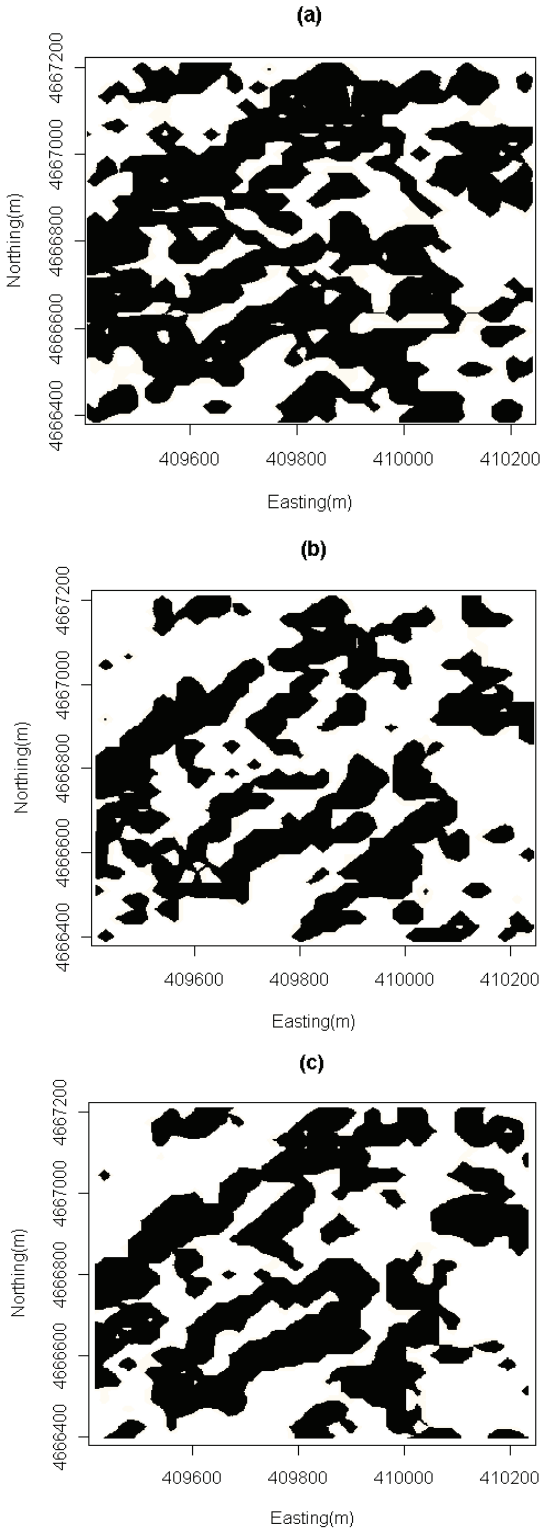

Figure 9. Shown in black are the areas that have value greater than 11. 21 Mg ha^{-1} year^{-1} (5 tons acre^{-1} year^{-1}) for erosion rate calculated using simulated DEMs using (a) RTK-DGPS measurements, (b) DF-DGPS measurements, and (c) USGS DEM dataset.

was substantially higher than 89.27 Mg ha^{-1} year^{-1} for the DF-DGPS DEM and 96.85 Mg ha^{-1} year^{-1} for the USGS DEM. For the RTK DEM, 95% of the grid erosion rates were smaller than 36.10 Mg ha^{-1} year^{-1}. For the DF-DGPS DEM and USGS DEM, 95% of the grid erosion rates were smaller than 25.93 Mg ha^{-1} year^{-1}. The smaller range of erosion rate estimates in the DF-DGPS and USGS DEMs relative to the RTK DEM signifies that, at some areas in the field, the erosion rate estimation using these DEMs was misleading.

To compare the erosion rate estimates using different DEMs, the percentage of the map area that has erosion rates greater than a tolerance, or *T* value, of 11.21 Mg ha^{-1} year^{-1} (5 tons acre^{-1} year^{-1} threshold) (Montgomery, 2007) was estimated. About 43% of the area in the erosion rate map estimated from the RTK DEM has values greater than the threshold (fig. 9a). The percentages of the area that has erosion rates greater than the threshold for the DF-DGPS DEM and USGS DEM were substantially lower: 24% and 27%, respectively (figs. 9b and 9c). The study shows that for accurate LS factor estimation to be used in the RUSLE equation for soil erosion rate estimation, high-accuracy elevation measurements, such as those acquired using RTK-DGPS receivers, are required. However, even more important than the estimated erosion rate is the uncertainty in that estimate, which may lead to an erosion rate associated with a conservation practice that is statistically indistinguishable from the *T* value. Hence, the modeler should take into account the uncertainty in the estimates by using uncertainty statistics to classify the areas that have unreliable estimations. This could provide guidelines for error reduction in management planning or conservation practice.

Uncertainty Estimates of Estimated Erosion Rate

A gray-scale map of the 95% CI of the 50 equiprobable erosion rates in each grid was constructed to describe the uncertainty in the erosion rate estimation (fig. 10). For the DEMs simulated from RTK-DGPS measurements, the 95% CI of the grid erosion rate was very small and ranged up to 8.09 Mg ha^{-1} year^{-1} (fig. 10a). For the DF-DGPS DEMs, the uncertainty of the estimated erosion rate in each grid was substantially higher than that of the RTK DEM, with 95% CI up to 83.74 Mg ha^{-1} year^{-1} (fig. 10b). This shows that even a small amount of elevation error in DEMs greatly affected the erosion rate estimates. Dark patches in many spots of the 95% CI map indicated high degrees of uncertainty in the estimates. The uncertainty in the erosion rate estimates was more clearly distinguished in the 95% CI map of the predicted erosion rate from the USGS DEM (fig. 10c). The high value of 95% CI in the erosion rate estimates is clearly observed in the areas that have large elevation error as computed in the error analysis. These areas were characterized in the northeast, middle, and southwest regions of the field, with 95% CI up to 109.81 Mg ha^{-1} year^{-1}. The low 95% CI of erosion rate estimates from the RTK DEM shows that the degree of certainty in the erosion rate estimates was higher using the RTK DEM compared to the DF-DGPS DEM and USGS DEM.

Similar to the average uncertainty of the elevation estimates, the average uncertainty of the erosion rate factor estimates across the study field was higher for the USGS DEM (table 1). Quantitatively, the average 95% CI estimates of the mean erosion rates across the field for the RTK DEM, DF-DGPS DEM, and USGS DEM were 0.54, 23.16, and 27.67 Mg ha^{-1} year^{-1}, respectively. Although the

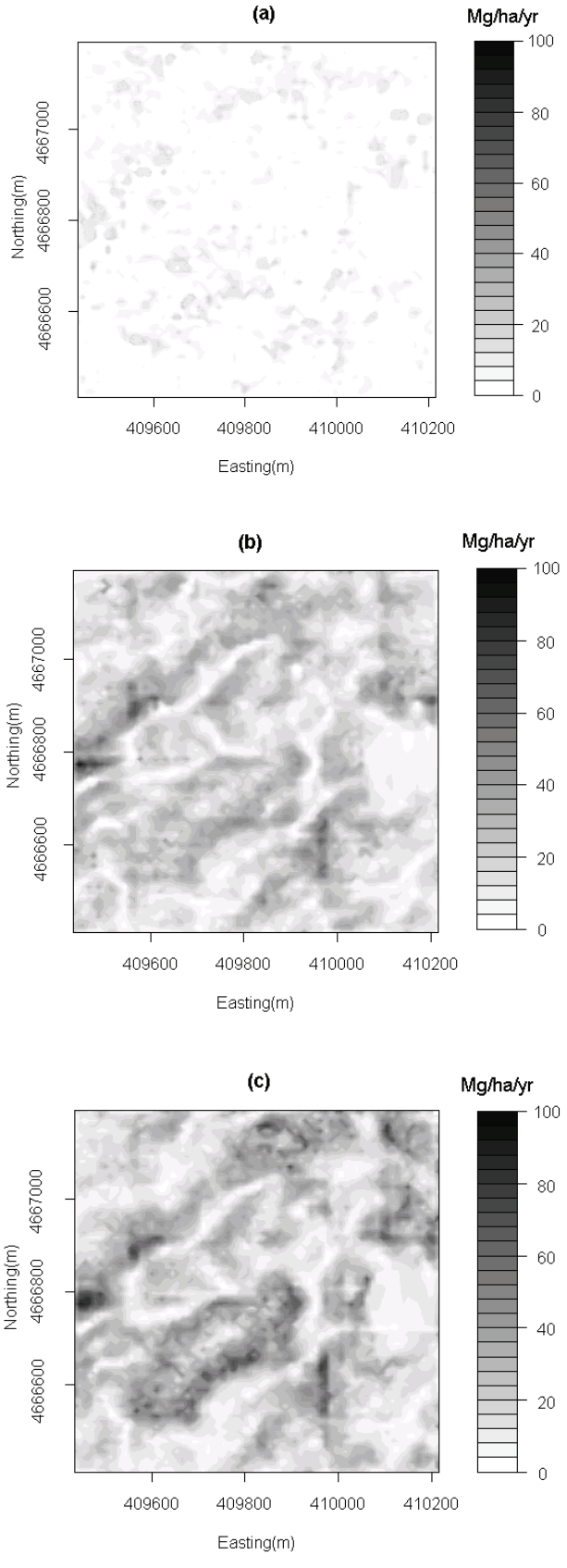

Figure 10. Gray-scale maps of 95% CI of erosion rate estimates calculated using 50 simulated DEMs using (a) RTK-DGPS measurements, (b) DF-DGPS measurements, and (c) USGS DEM dataset.

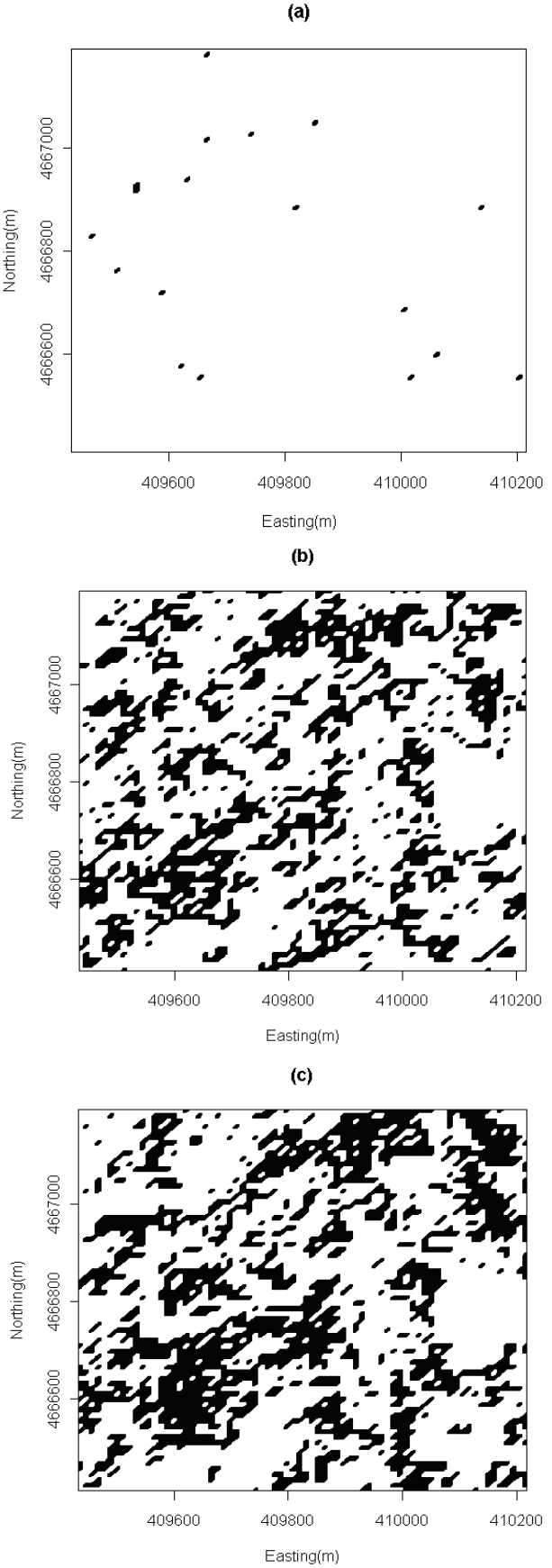

Figure 11. Shown in black are the areas that have erosion rate estimates with CIs containing the *T* value of 11. 21 Mg ha^{-1} year^{-1} (5 tons acre^{-1} year^{-1}) for DEMs developed using (a) RTK-DGPS measurements, (b) DF-DGPS measurements, and (c) USGS DEM dataset.

elevation errors in the DF-DGPS DEM were smaller than those in the USGS DEM, the impact of the errors on erosion rate estimation was substantially higher. More than 80% of the area in the erosion rate map predicted from the DF-DGPS DEM and USGS DEM has 95% CI greater than 11.21 Mg ha^{-1} year^{-1} (5 tons acre^{-1} year^{-1}).

In this study, if the erosion rate tolerance, or *T* value, were set to 11.21 Mg ha^{-1} year^{-1} (5 tons acre^{-1} year^{-1}) as a threshold (Montgomery, 2007), then about 31% of the erosion rate estimates using the DF-DGPS DEM and 35% of the erosion rate estimates using the USGS DEM were statistically indistinguishable from the *T* value. In other words, more than 30% of the area in the erosion rate CI map predicted from the DF-DGPS DEM and USGS DEM contained the *T* value (fig. 11). This means that it cannot be determined if the estimated erosion rate was statistically different from the *T* value, and hence it is difficult to use the best-informed conservation measures at those locations. Overall, the uncertainty estimators, such as the 95% CI of the erosion rate estimates, which were calculated on grid-by-grid basis, enabled quantification and visualization of the impacts of the DEM errors in the erosion rate estimation.

Thorough evaluation of the uncertainty in the elevation data is needed for drawing appropriate conclusions on the impact of the DEM errors on erosion rate estimation. The quantification of the uncertainty estimators on a grid-by-grid basis enables more precise assessment of reliability of the estimated estimates across the study area. One current problem is that there is no standard uncertainty statistic in the spatial estimation of elevation data. This study used 95% confidence intervals; future analysis could focus on what is the best way to communicate "uncertainty" in spatial data estimation, which is critical for precise assessment of reliability of the estimates.

CONCLUSION

The uncertainty in the estimated DEMs affected erosion rate estimation in this study. From this study, the following conclusions can be drawn:

- The average elevation uncertainty for the DF-DGPS DEM and USGS DEM were of similar magnitude and substantially higher than that of the RTK DEM by about an order of magnitude. Although the errors in the DF-DGPS measurements were smaller (ranging from -3.14 to 4.76 m) than the errors in the USGS DEM dataset (ranging from -7.04 to 8.45 m), the impact of these errors in the DEM elevation uncertainty were substantial.
- Even small uncertainties in the DEM elevation produced large uncertainty in the average annual erosion rate estimates in the study field. More than 30% of the area in the erosion rate CI map predicted from the DF-DGPS DEM and USGS DEM contained the *T* value of 11.21 Mg ha^{-1} year^{-1} (5 tons acre^{-1} year^{-1}).
- Quantifying uncertainty using a statistic such as 95% CI in each grid enables a thorough assessment of the estimation uncertainty. The uncertainty estimators that were calculated on a grid-by-grid basis provided visualization of the impacts of the DEM errors in the erosion rate estimation.

This study focused on DEM uncertainty associated with elevation values and its effect on erosion rate estimates. DEM uncertainty also exists due to spatial resolution, and its effects may be different but coexisting in all DEMs. Uncertainty due to spatial resolution coupled with elevation uncertainty may have substantial effects, and thus should be investigated in future studies.

The practical implementation of this study is mainly for the assessment of conservation practices in an agricultural field. This study showed that less accurate elevation data may lead to erosion rate estimates that are uncertain (relative to the RTK DEM) in areas where this information is most critical from a conservation standpoint. For the purposes of precision conservation, areas of the field that have erosion rates high enough for concern should be targeted. However, if less accurate data lead to estimates that have large confidence intervals, then it is difficult to implement the best-informed conservation measures at those locations.

REFERENCES

Carlisle, B. H. 2005. Modeling the spatial distribution of DEM error. *Trans. GIS* 9(4): 521-540.

Carrara, A., G. Bitelli, and R. Carla. 1997. Comparison of techniques for generating digital terrain models from contour lines. *Intl. J. Geograph. Info. Sci.* 11(5): 451-473.

Ehlschlaeger, C. R., and A. Shortridge. 1997. Modelling elevation uncertainty in geographical analyses. In *Proc. 7th Intl. Symp. Spatial Data Handling*, 585-595. M. J. Kraak and M. Molenaar, eds. London, U.K.: Taylor and Francis.

Fangmeier, D. D., W. J. Elliot, S. R. Workman, R. L. Huffman, and G. O. Schwab. 2006. *Soil and Water Conservation Engineering*. 5th ed. New York, N.Y.: Thomson Delmar Learning.

Gao, J. 1997. Resolution and accuracy of terrain representation by grid DEMs at micro-scale. *Intl. J. Geograph. Info. Sci.* 11(2): 199-212.

GeoCommunity. 2007. USGS DEM Resources: 1995-2007. GIS Data Depot. Niceville, Fla.: MindSites Group, LLC. Available at: http://data.geocomm.com. Accessed 23 April 2006.

Goovaerts, P. 1997. *Geostatistics for Natural Resources Evaluation*. New York, N.Y.: Oxford University Press.

Holmes, K. W., O. A. Chadwick, and P. C. Kyriakidis. 2000. Error in a USGS 30-meter digital elevation model and its impact on terrain modeling. *J. Hydrol.* 233(1-4): 154-173.

Hoyos, N. 2005. Spatial modeling of soil erosion potential in a tropical watershed of the Colombian Andes. *Catena* 63(1): 85-108.

Hunter, G. J., and M. F. Goodchild. 1997. Modeling the uncertainty of slope and aspect estimates derived from spatial databases. *Geograph. Analysis* 29(1): 35-49.

Hunter, G. J., M. Caetano, and M. F. Goodchild. 1995. A methodology for reporting uncertainty in spatial database products. *URISA J.* 7(2): 11-21.

Isaaks, E. H., and R. M. Srivastava. 1989. *An Introduction to Applied Geostatistics*. New York, N.Y.: Oxford University Press.

Karkee, M., B. L. Steward, and S. Abd Aziz. 2008. Improving quality of digital elevation models through data fusion. *Biosystems Eng.* 101(3): 293-305.

Kyriakidis, P. C., A. M. Shortridge, and M. F. Goodchild. 1999. Geostatistics for conflation and accuracy assessment of digital elevation models. *Intl. J. Geograph. Info. Sci.* 13(7): 677-707.

Lee, G. S., and K. H. Lee. 2006. Scaling effect for estimating soil loss in the RUSLE model using remotely sensed geospatial data in Korea. *Hydrol. Earth Syst. Sci.* 3(1): 135-157.

Lu, D., G. Li, G. S. Valladares, and M. Batistella. 2004. Mapping soil erosion risk in Rondonia, Brazilian Amazonia: Using RUSLE, remote sensing, and GIS. *Land Degrad. and Develop*. 15(5): 499-512.

McCool, D. K, G. R. Foster, and G. A. Weesies. 1997. Slope length and steepness factors (LS). In *Predicting Soil Erosion by Water: A Guide to Conservation Planning with the Revised Universal Soil Loss Equation (RUSLE)*, 101-251. Agriculture Handbook No. 703. Renard, K. G., G. R. Foster, G. A. Weesies, D. K. McCool, and D. C. Yoder, eds. Washington, D.C.: USDA Agricultural Research Service.

Mitasova, H., W. M. Brown, M. Hohmann, and S. Warren. 2001. Using soil erosion modeling for improved conservation planning: A GIS-based tutorial. Urbana-Champaign, Ill.: University of Illinois, Geographic Modeling Systems Laboratory. Available at: http://skagit.meas.ncsu.edu/~helena/gmslab/reports/CerlErosionTutorial/denix/default.htm. Accessed 23 July 2008.

Montgomery, D. R. 2007. Soil erosion and agricultural sustainability. *Proc. Natl. Acad. of Sci.* 104(33): 13268-13272.

Renard, K. G., G. R. Foster, G. A. Weesies, D. K. McCool, and D. C. Yoder, eds. 1997. *Predicting Soil Erosion by Water: A Guide to Conservation Planning with the Revised Universal Soil Loss Equation (RUSLE)*. Agriculture Handbook No. 703. Washington, D.C.: USDA Agricultural Research Service.

Renschler, C. S., and D. C. Flanagan. 2008. Site-specific decision-making based on RTK GPS survey and six alternative elevation data sources: Soil erosion predictions. *Trans. ASABE* 51(2): 413-424.

Renschler, C. S., D. C. Flanagan, and B. A. Engel. 2001. Data accuracy issues in spatially distributed soil erosion modeling: What does decision-making gain? ASAE Paper No. 701P0007. St. Joseph, Mich.: ASAE.

Sheskin, D. 2004. *Handbook of Parametric and Nonparametric Statistical Procedures*. 3rd ed. Boca Raton, Fla.: Chapman and Hall/CRC

Trangmar, B. B., R. S. Yost, and G. Uehara. 1985. Application of geostatistics to spatial studies of soil properties. *Advances in Agron.* 38: 45-94.

USDA. 2008. *User's Reference Guide: Revised Soil Loss Equation Version 2 (RUSLE2)*. Washington, D.C.: USDA National Agricultural Research Service. Available at: www.ars.usda.gov. Accessed 14 October 2008.

USGS. 1998. Standard for digital elevation models: Part 2. Specifications. Reston, Va.: U.S. Geological Survey. Available at: http://nationalmap.gov/standards/demstds.html. Accessed 30 October 2008.

Wischmeier, W. H., and D. D. Smith. 1965. *Predicting Rainfall-Erosion Losses from Cropland East of the Rocky Mountains*. Agricultural Handbook No. 282. Washington, D.C.: USDA Agricultural Research Service.

Wise, S. M. 1998. The effect of GIS interpolation errors on the use of digital elevation models in geomorphology. In *Landform Modelling and Analysis*, 139-164. S. N. Lane, K. S. Richards, and J. H. Chandler, eds. Chichester, U.K.: John Wiley and Sons.

Wechsler, S. P. 2007. Uncertainties associated with digital elevation models for hydrologic applications: A review. *Hydrol. Earth Syst. Sci*. 11(4): 1481-1500.

Wechsler, S. P., and C. N. Kroll. 2006. Quantifying DEM uncertainty and its effect on topographic parameters. *Photogram. Eng. and Remote Sensing* 72(9): 1081-1090.